

“Staircase” Saccadic Intrusions plus Transient Yoking and Neural Integrator Failure Associated with Cerebellar Hypoplasia: A Model Simulation

Janet C. Rucker

The Daroff-Dell’Osso Ocular Motility Laboratory, Louis Stokes Cleveland Veterans Affairs Medical Center and CASE Medical School and the Departments of Neurology, and Ophthalmology, Case Western Reserve University and University Hospitals of Cleveland, Cleveland, OH; Department of Neurology, Rush University, Chicago, IL

Louis F. Dell’Osso

The Daroff-Dell’Osso Ocular Motility Laboratory, Louis Stokes Cleveland Veterans Affairs Medical Center and CASE Medical School and the Departments of Neurology, and Biomedical Engineering, Case Western Reserve University and University Hospitals of Cleveland, Cleveland, OH

Siobhan Garbutt

The Daroff-Dell’Osso Ocular Motility Laboratory, Case Western Reserve University and University Hospitals of Cleveland, Cleveland, OH; Department of Physiology, Keck Center for Integrative Neuroscience, University of California, San Francisco, San Francisco CA

Jonathan B. Jacobs

The Daroff-Dell’Osso Ocular Motility Laboratory, and Louis Stokes Cleveland Veterans Affairs Medical Center and CASE Medical School and the Departments of Neurology, Case Western Reserve University and University Hospitals of Cleveland, Cleveland, OH

This work was supported in part by the Office of Research and Development, Medical Research Service, Department of Veterans Affairs.

Presented in part at the 2003 North American Neuro-Ophthalmology Society (NANOS) and Association for Research in Vision and Ophthalmology (ARVO) meetings.

Address correspondence to
L. F. Dell’Osso, Ph.D., Director,
Daroff-Dell’Osso Ocular Motility Laboratory,
Louis Stokes Cleveland DVA Medical Center,
10701 East Boulevard, Cleveland, OH 44106,
USA. E-mail: lfd@case.edu

ABSTRACT We present hypothesized ocular motor mechanisms of unique “staircase-like” sequences of saccadic intrusions in one direction that we have named, “staircase saccadic intrusions (SSI),” square-wave jerks/oscillations (SWJ/SWO), and transient failures of yoking and neural integrators in a patient with severe hypotonia, ataxic speech, motor and language developmental delays, and torticollis (Joubert syndrome). Brain magnetic resonance imaging showed hypoplasia of the cerebellar vermis and inferior cerebellar peduncles, abnormal superior cerebellar peduncles with deepening of the interpeduncular fossa, and enlargement of the fourth ventricle. During far and near fixation and smooth pursuit (rightward markedly better than leftward), the subject exhibited conjugate SSI (rightward more than leftward, with intersaccadic intervals equivalent to the normal 250 msec visual latency), SWJ, SWO, and uniocular, convergent and divergent saccades (including double saccades). Simulations using a behavioral ocular motor system model identified hypothetical mechanisms for SWJ, SWO, and SSI and ruled out the loss of efference copy as the cause. SSI may result from simultaneous dysfunctions: 1) a transient loss of accurate retinal-error information and/or sampled, reconstructed error; plus 2) a constant sampled, reconstructed retinal error that drives saccades.

KEYWORDS saccadic intrusions, yoking, neural integrator, cerebellar hypoplasia, model

INTRODUCTION

Studies of individual occurrences of ocular motor dysfunction often allow insights into underlying ocular motor system mechanisms. In this patient, we had to identify the clinical characteristics and diagnosis, determine the nature and, if possible, causes of his saccadic intrusions and other ocular motor signs.

The triad of thick, straight superior cerebellar peduncles, deepening of the interpeduncular fossa, and cerebellar vermis hypoplasia is characteristic of the “molar tooth sign,” thought to be due to non-decussation of the superior cerebellar peduncles.^{1,2} Although not pathognomonic, it is highly suggestive of Joubert

syndrome.³ This rare syndrome, initially described by the Canadian Neurologist Marie Joubert in 1969⁴ has a prevalence of 1 in 100,000 and is comprised of cerebellar vermis hypoplasia (usually with the “molar tooth sign” on magnetic resonance imaging, MRI), hypotonia, developmental delay, an abnormal breathing pattern with alternating apneas and hyperpneas, and abnormal ocular motility with phenotypic variability.^{5–7}

This study of a patient with specific, identifiable cerebellar lesions resulted in the discovery of a new, never before recorded or described saccadic intrusion. Because of its “staircase-like” appearance in ocular motor recordings, we named it a “staircase” saccadic intrusion (SSI). These intrusions appeared along with (but distinct from) square-wave jerks/oscillations (SWJ/SWO) in a patient with cerebellar dysfunction. The patient also exhibited uniocular saccades, convergent saccades, and divergent saccades, including double saccades. Using a behavioral ocular motor system (OMS) model,^{8,9} we were able to hypothesize mechanisms within the normal saccadic subsystem that reproduced both the common SWJ and SWO seen in normals and many patients, and this rare SSI. The staircase intrusions may result from a failure of the saccadic system to properly use visual information to correct eye position (e.g., the sign of retinal feedback might be transiently reversed or a constant internal position error created). The clinical relevance of determining the mechanism lies in both its consistency with the rarity of the condition and in its relationship to more common saccadic intrusions.

Case Description

The patient was the product of a full-term gestation, complicated by premature labor that was stopped iatrogenically. He initially came to neurologic attention at 27 months of age, at which time he underwent evaluation for developmental delay. He had delay of motor milestones: sitting at 9 months, crawling at 12 months, pulling to a stand at 26 months, and walking with assistance at the time of evaluation. Language milestones were also delayed. He had severe hypotonia and required a truncal brace for support. His clinical chart indicated that he had “ocular motor apraxia” with “difficulty following an object in all directions.” At age 3 a “fine nystagmus” and from age 4 a normal fundus examination were noted. At age 8, he exhibited “head shaking, wandering eye movements, a left head tilt, and right head turn.” At age 9, he was in third grade with “mathe-

matic difficulty” and had poor motor coordination and ataxic speech. He was sent to our ocular motility laboratory for evaluation of “ocular motor apraxia” at that age, when we first examined him and performed MRI and ocular motor studies. Brain MRI with gadolinium revealed hypoplasia of the cerebellar vermis and inferior cerebellar peduncles, abnormal superior cerebellar peduncles with deepening of the interpeduncular fossa, and enlargement of the fourth ventricle (Figure 1). The appearance of the findings at the level of the superior cerebellar peduncles is consistent with the previously described “molar tooth sign” (Figure 1-Top), the significance of which will be discussed below.^{1,7} There was no abnormal gadolinium enhancement.

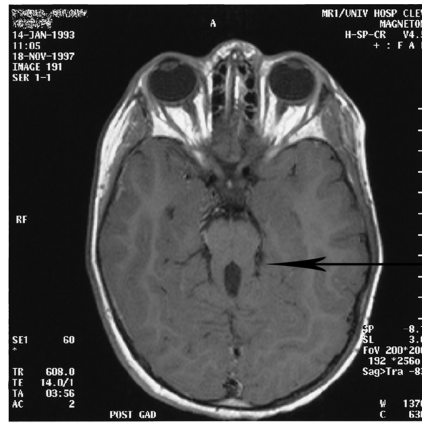
METHODS

Subjects and Protocol

Written consent was obtained from the subject’s parents before testing. All test procedures were carefully explained to the subject and his parents before the experiment began, and were reinforced with verbal commands during the trials. The subject was seated in a chair with headrest and chin stabilizer, far enough from an arc of red LEDs to prevent convergence effects (>5 feet). At this distance the LED subtended less than 0.1° of visual angle. The room light could be adjusted from dim down to blackout to minimize extraneous visual stimuli.

Recording

Infrared reflection was used to record the eye movements of this subject. The infrared reflection system (Applied Scientific Laboratories, Waltham, MA) was linear to 20° in the horizontal plane and monotonic to 25–30° with a sensitivity of 0.25°. The total system bandwidth (position and velocity) was 0–100 Hz. The data were digitized at 500 Hz with 16-bit resolution. The IR signal for each eye was calibrated with the other eye behind cover to obtain accurate position information; the foveation periods were used for calibration. Eye positions and velocities (obtained by analog differentiation of the position channels) were displayed on a strip chart recording system (Beckman Type R612 Dynograph). Eye movements were studied on two separate occasions during fixation at gaze angles varying between ±30° and at convergence angles ranging from far to 20D and during smooth pursuit at velocities of 5–40°/sec.



T1-Coronal

“Molar-tooth” sign of thickened superior cerebellar peduncles



T2-Sagittal

Atrophy of the superior cerebellum

Enlargement of the 4th ventricle, indicating atrophy of the cerebellar vermis

FIGURE 1 (Top) T1-weighted axial brain MRI reveals thickened, straightened bilateral superior cerebellar peduncles (arrow) with deepening of the interpeduncular fossa due to cerebellar vermis hypoplasia. This appearance is consistent with the “molar tooth sign” (see text for discussion). (Bottom) T2-weighted sagittal brain MRI reveals enlargement of the fourth ventricle and cerebellar atrophy (arrow).

Analysis

All the analysis and graphical plots were done in MATLAB environment (The MathWorks, Natick, MA) using custom-written software (OMtools, available from <http://www.omlab.org>). Only eye position was sampled directly; velocity was derived from the position data by a fourth-order central-point differentiator; acceleration was derived from the velocity data by the same differentiator. Position data were pre-filtered with a low-pass filter with the cutoff frequency of 50 Hz to reduce the noise while minimally affecting the data.

Definitions

The following definitions are used in this paper:

Saccades

- Convergent Saccades (C-S), simultaneous adducting saccades in both eyes

- Divergent Saccades (D-S), simultaneous abducting saccades in both eyes
- Vergence-unequal-interocular-amplitude saccades, either converging (cs) or diverging (ds)
- Uniocular Saccades (us), saccade in one eye while the other is either still or makes a small double saccadic pulse (DSP)

Saccadic Intrusions and Oscillations

- Double Saccadic Pulse, two back-to-back (i.e., no intersaccadic latency) saccades of equal amplitudes in opposite directions
- Flutter, multiple back-to-back (i.e., no intersaccadic latency) saccades
- Square-Wave Jerk/Oscillation, two/multiple back-to-back (i.e., normal intersaccadic latency) equal-amplitude saccades in opposite directions
- Staircase Saccadic Intrusions (SSI), “staircase-like” sequences of saccades in one direction that interrupt fixation or smooth pursuit

TABLE 1A Right-Eye Staircase Saccadic Intrusions

Stimulus Fixation	Intrusions Right	Intrusions Left	Average N° Steps R	Average N° Steps L	Intrusions/min	Steps/min
Trial 1	50%	50%	3	3	27	82
Trial 2	62%	38%	3	2.5	31.5	93
Trial 3	67%	33%	3	2.5	27	73
Trial 4	63%	37%	3.5	2.5	32.5	101
Average ± SE Pursuit	60.5 ± 3.7	39.5 ± 3.7	3 ± 0.1	2.5 ± 0.1	29.5 ± 1.5	87.5 ± 6.1
5°/s	75%*	25%*	3	2*	37.5*	100*
10°/s	78%*	22%*	4*	2.5	27	97.5
20°/s	62.5%	37.5%	4.5*	3	29	109*
40°/s	100%*	0%*	4.5*	0*	24*	110*

RIGHT EYE all conditions: R staircase : L staircase = 70% : 30%; Average number of steps per staircase: 3; 29.5 intrusions/min; 96 steps/min.

*Outside 95% confidence limits for values recorded during fixation.

Other

- Neural Integrator Leak, decelerating drift of the eye back towards primary position
- Nystagmus (Jerk), slow eye movements reset by oppositely directed fast phases (saccades); the saccades may be conjugate (jerk right, JR or jerk left, JL) or any of the above types (e.g., C-SJ, JL_{ds}, or JR_{us})

RESULTS

Ocular Motor Findings

Fixation

Fixation on a stationary target was interrupted by a series of unidirectional saccades, or “staircase” saccadic intrusions (SSI) (28/min), more often to the right (54% of the time) than to the left (46%). There was an average of 3 saccades (steps) per each staircase

intrusion. Saccades could be unequal (e.g., within each staircase) or disconjugate (e.g., divergent nystagmus). There were also: frequent (10/min) SWJ and SWO; occasional bursts of flutter that were disconjugate and of variable interocular phase; centripetal drift of either eye; and variable strabismus. Figure 2 shows examples of SSI, SWJ, SWO, flutter, uni- and binocular neural integrator failure, and divergent saccades during fixation of a stationary, primary-position target. Table 1 summarizes the characteristics of the SSI for both eyes during fixation and smooth pursuit.

Smooth Pursuit

Smooth pursuit was absent to left and of low gain to the right ($G \leq 0.78$ at 5 deg/s, 0.62 at 10 deg/s, 0.47 at 20 deg/s and 0.16 at 40 deg/s). It was also interrupted by the above-described saccadic intrusions; the frequency of saccadic intrusions increased (43/min). Figure 3 shows

TABLE 1B Left-Eye Staircase Saccadic Intrusions

Stimulus Fixation	Intrusions Right	Intrusions Left	Average N° Steps R	Average N° Steps L	Intrusions/min	Steps/min
Trial 1	50%	50%	3.5	3.5	23	79
Trial 2	56%	44%	3.5	2.5	27.5	85
Trial 3	62%	38%	3	2.5	29	80.5
Trial 4	56%	44%	3.5	3	28.5	91.5
Average ± SE Pursuit	56 ± 2.4	44 ± 2.4	3.5 ± 0.1	3 ± 0.2	27 ± 1.4	84 ± 2.8
5°/s	73.5%*	26.5%*	3	2*	29	85.5
10°/s	81%*	19%*	4*	2*	24	84
20°/s	62.5%*	37.5%*	4.5*	3	29	109*
40°/s	74%*	26%*	4*	2.5	42*	133*

LEFT EYE all conditions: R staircase : L staircase = 64% : 36%; Average number of steps per staircase: 3; 29 intrusions/min; 93.5 steps/min.

*Outside 95% confidence limits for values recorded during fixation.

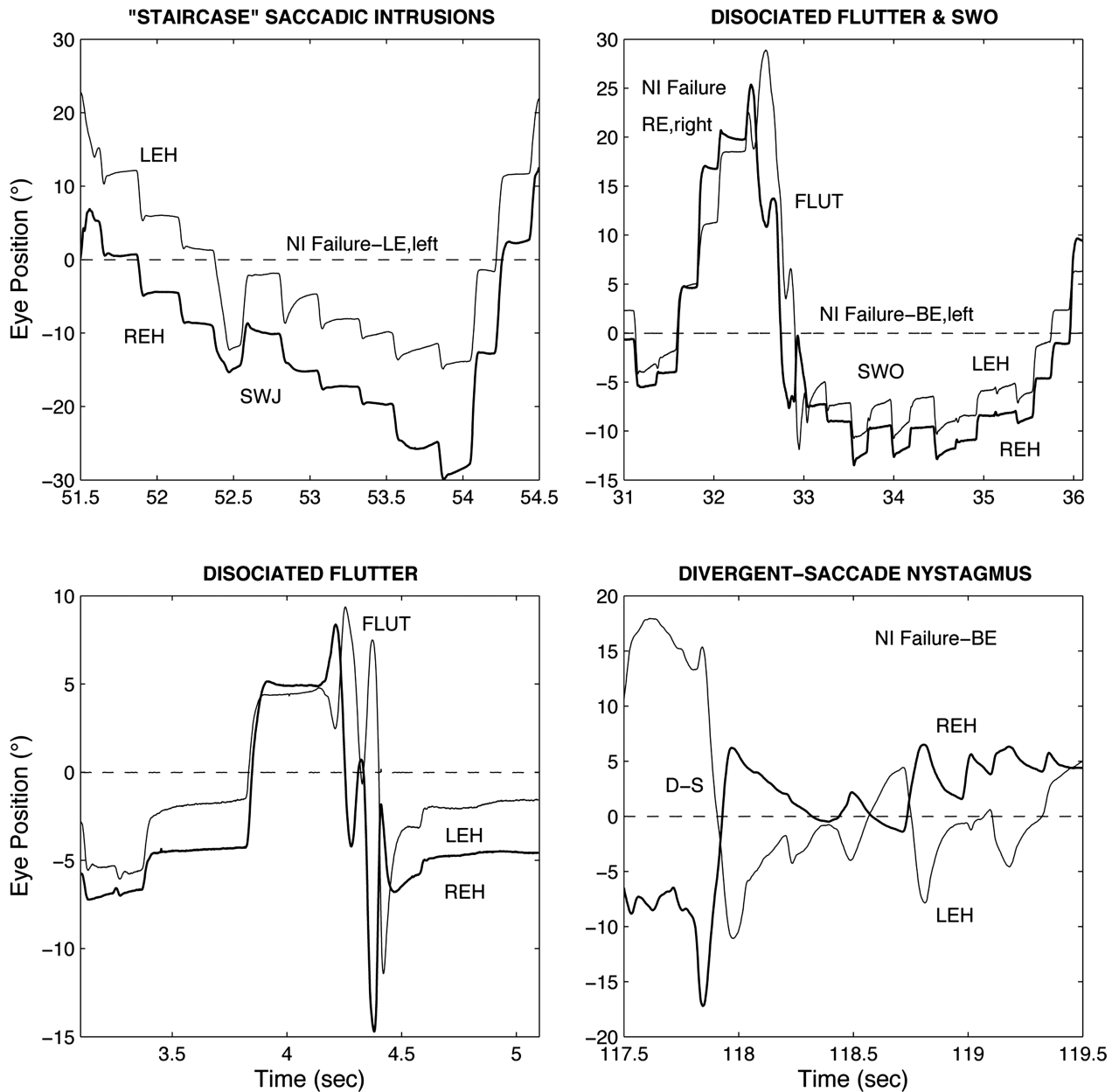


FIGURE 2 Examples of the subject's ocular motor disorders during attempted fixation of a target in primary position. (Top left) Leftward, equal-step SSI including a leftward SWJ and unocular neural integrator leak of the left eye in left gaze (LE,left). (Top right) Rightward, unequal-step SSI with unocular neural integrator leak of the right eye in right gaze (RE,right) followed by flutter during the refixation and SWO with neural integrator leak of both eyes in left gaze (BE,left). (Bottom left) Rightward, unequal-step SSI followed by divergent flutter during the refixation. (Bottom right) Divergent-saccade (D-S) followed by D-S nystagmus with neural integrator leak of both eyes. In this and Figures 3 and 4, REH-right eye horizontal (heavy trace), LEH-left eye horizontal (thin trace), FLUT-flutter, and both eyes were viewing.

examples of SSI, SWJ, flutter, and unocular saccades during smooth pursuit of targets moving at 5, 10, 20, and 40°/sec.

Disconjugate Eye Movements

During fixation of stationary targets, or refixation from one stationary target to another, disconjugate eye movements were evident. Figure 4 shows examples of converging (cs), divergent (D-S), and unocular (us)

saccades, as well as a double saccadic pulse made (DSP) during fixation of targets at 30° left gaze (Top) and in primary position (Middle and Bottom). Note that the time scale identifies these as saccades, as do their high velocities (not shown). Because they occurred during steady fixation of a single stationary target, they are not version-vergence saccades, and are abnormal, despite having normal dynamics (i.e., peak velocities and durations).

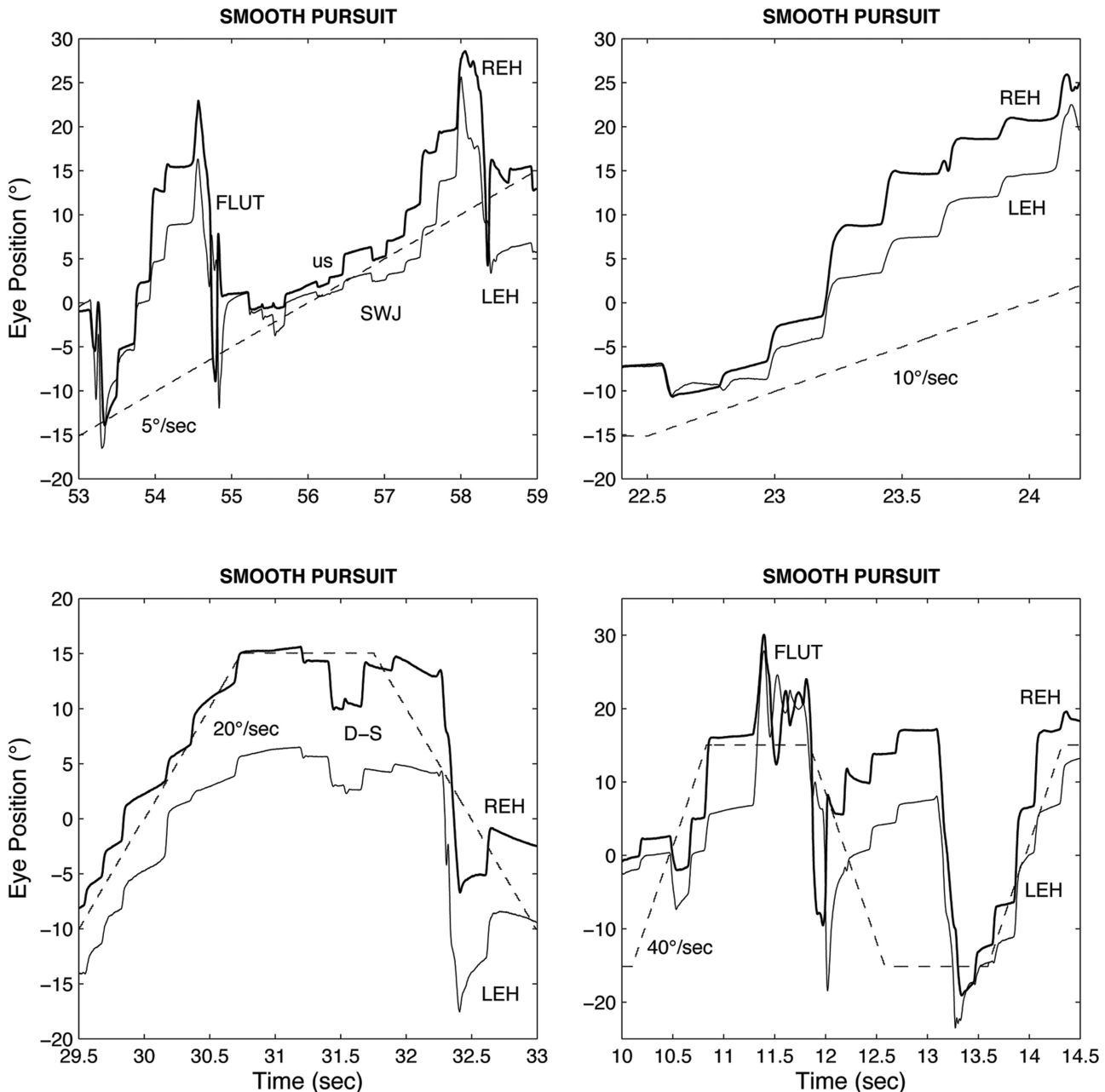


FIGURE 3 Examples of the subject's ocular motor disorders during attempted smooth pursuit of a target moving at different constant velocities. (5°/sec) Rightward, unequal-step SSI followed by flutter during refixation, good pursuit including a uniocular saccade (us) and a SWJ, another rightward, unequal-step SSI, and then refixation. (10°/sec) Rightward, unequal-step SSI following good pursuit. (20°/sec) Rightward, unequal-step SSI during low-gain rightward pursuit, divergent saccades (D-S) during rightward fixation, and saccadic, low-gain pursuit to the left. (40°/sec) Saccadic, low-gain rightward pursuit, flutter during rightward fixation, saccadic, low-gain leftward pursuit interrupted by a rightward unequal SSI, refixation, and a rightward, unequal-step SSI during low-gain rightward pursuit.

Ocular Motor System (OMS) Model Simulations

Functional ocular motor models provide a strict structure within which hypothetical mechanisms for dysfunction may be tested. The simulations for the SSI, SWJ, and SWO were made using a behavioral OMS model.⁹ Modifications in the form of transient "noise"

in key signals were made within the Internal Monitor portion of the model where target, eye, and motor-error signals are reconstructed using retinal error signals and efference copy of eye position.

Staircase Saccades in Normals

Normals can be induced to make a series of staircase saccades in response to a target displacement by

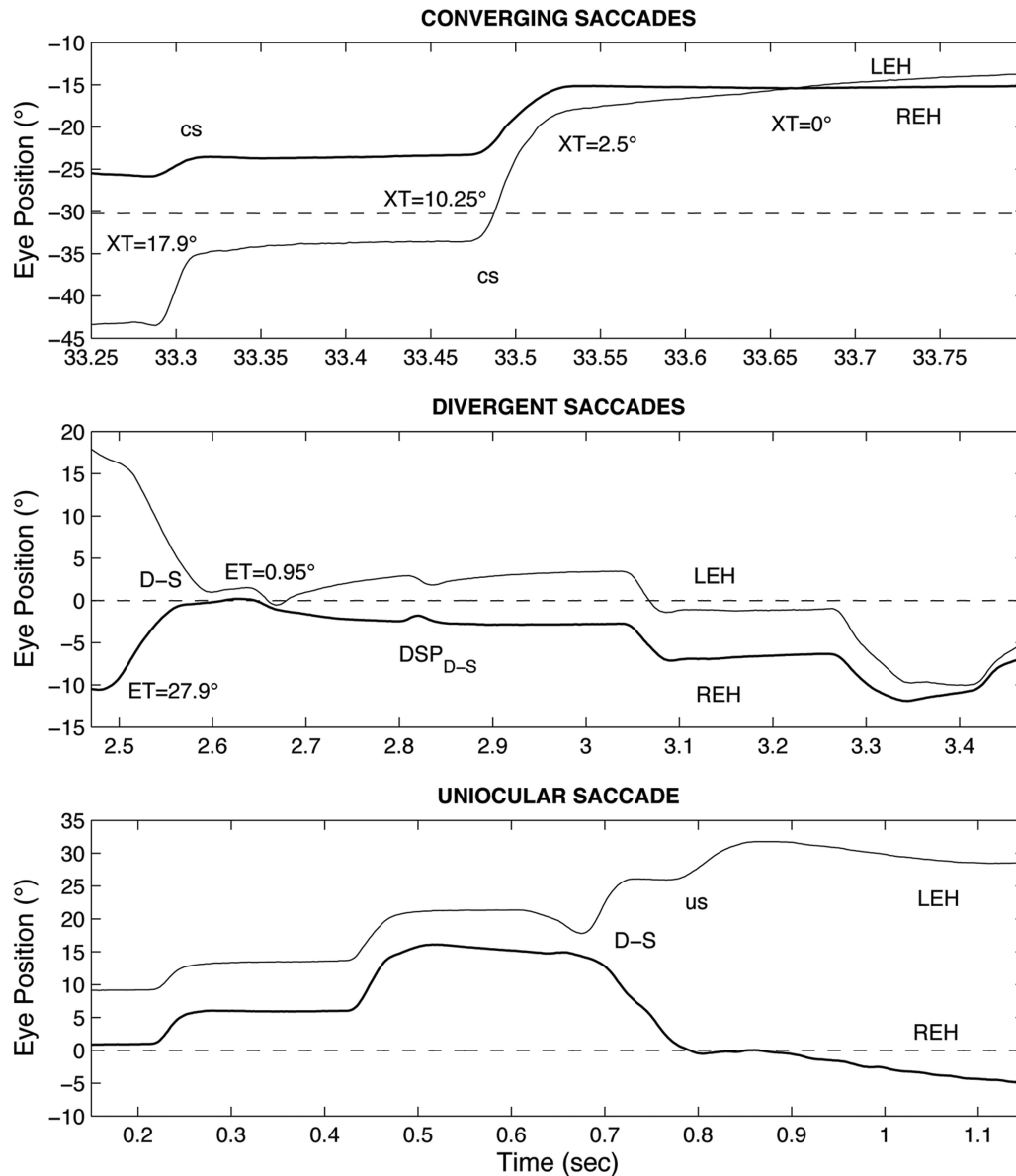


FIGURE 4 Examples of the subject's disconjugate ocular motor disorders during attempted fixation of a target in primary position. (Top) Two "converging" rightward saccades (cs) that eliminate a 17.9° exotropia. (Middle) A "divergent" saccade (D-S) to eliminate a 27.9° esotropia, a divergent double saccadic pulse (DSP_{D-S}), and a conjugate leftward saccade. (Bottom) Two rightward conjugate saccades followed by a D-S and a rightward unioocular saccade (us) of the left eye.

opening the retinal feedback loop. This is accomplished easily by using a signal measuring the eye's response to the initial target displacement to further displace the target. Figure 5a shows the OMS model with such an external feedback loop. This causes the target to step off in one direction as the eye attempts to catch it with a series of staircase saccades. Mechanistically, this maneuver creates a constant retinal error signal and the ocular motor system responds to it with its characteristic latency of 200–250 ms.

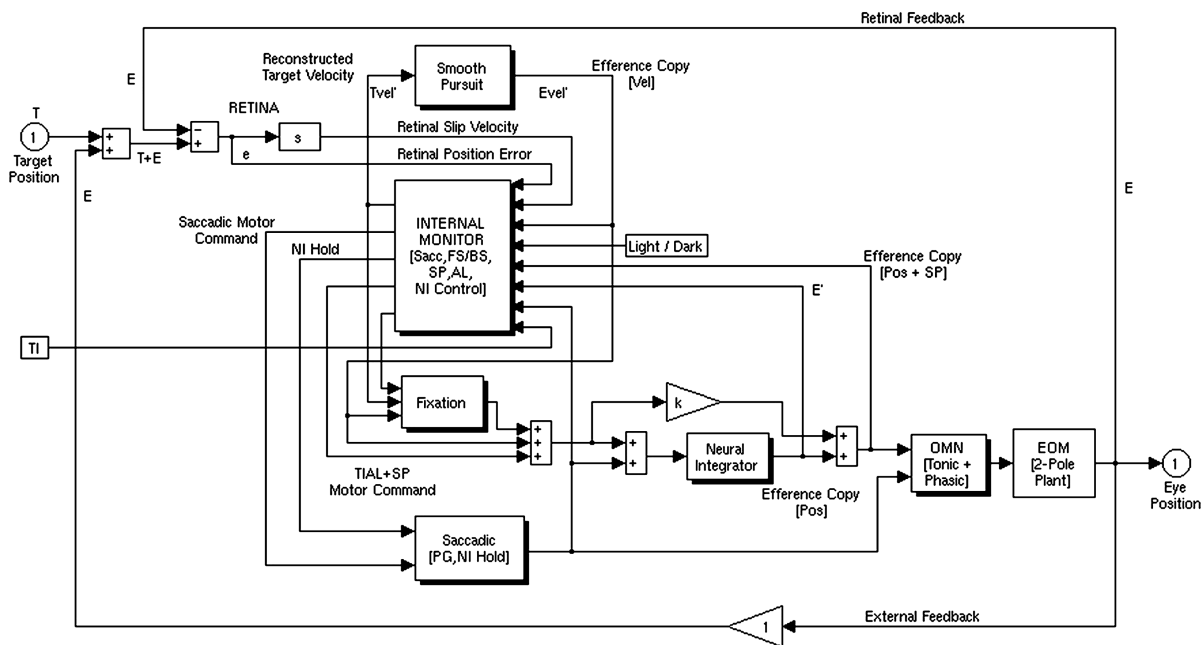
The relevant portion of the OMS model is shown darkened in Figure 5b where operations contained

within the Internal Monitor are exploded out for easier inspection; the full details of the functions in the Internal Monitor may be found in prior publications.^{8,9} or downloaded from our website, www.omlab.org.

Role of Efference Copy in the Internal Monitor

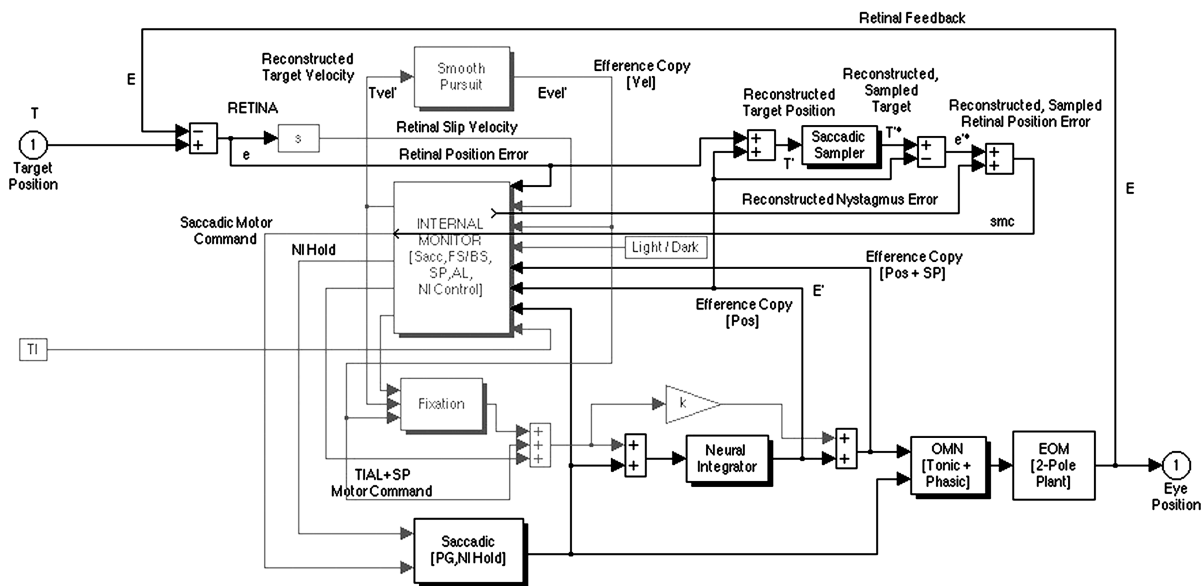
In the OMS model (see Figure 5b), actual target position (T) is approximated by reconstructed target position (T') by adding efference copy of presumed eye position (E') to retinal error (e). That is, perceived target position, $T' = e + E'$, where e is determined optically at the

OMS Block Diagram with External Feedback



(a)

OMS Block Diagram: Saccadic Foundations



(b)

FIGURE 5 (a) Behavioral ocular motor system (OMS) model with external feedback of eye position to change the effective retinal feedback from its value of -1.0 . The major subsystems and functional blocks of this behavioral model are shown with their interconnections. (b) OMS model with an expanded view (dark lines) of the portion of the relevant functional circuitry within the Internal Monitor that is responsible for target reconstruction from retina error and efference copy of eye position, reconstructed sampled target position (i.e., perceived target position), reconstruction of retinal position error (sampled), and generation of the saccadic motor command after accounting for internally generated eye movement (e.g., nystagmus).

retina as $T - E$. T' is then sampled, producing T'^* . Note that in the presence of nystagmus, E contains the nystagmus signal, N (i.e., it is the actual eye position signal, E plus the nystagmus signal, N). Thus, e also contains N ,

albeit as $-N$. Retinal error is approximated internally by sampled, reconstructed retinal error (e'^*), calculated as

$$e'^* = T'^* - E' = (e + E')^* - E' = e^*$$

and the saccadic motor command (smc) is produced from

$$\text{smc} = e^{/*} + N'$$

where N' is reconstructed nystagmus needed to cancel the $-N$ signal contained in $e^{/*}$. It is smc that drives the pulse generator to make an appropriate saccade to the target, thereby eliminating errors due to any internal ocular motor oscillation (saccadic or nystagmus).

“Staircase” Saccadic Intrusions (SSI)

Our initial attempt to simulate SSI was to transiently disable the efference copy signal to induce a constant retinal error signal similar to that caused by the use of external feedback in normals. Figure 6 shows the resulting simulated SSI in normals when retinal feedback is externally canceled (Top). The intersaccadic intervals are equal to the normal saccadic latency of 250 msec, mimicking the eye movements of normals. However, when

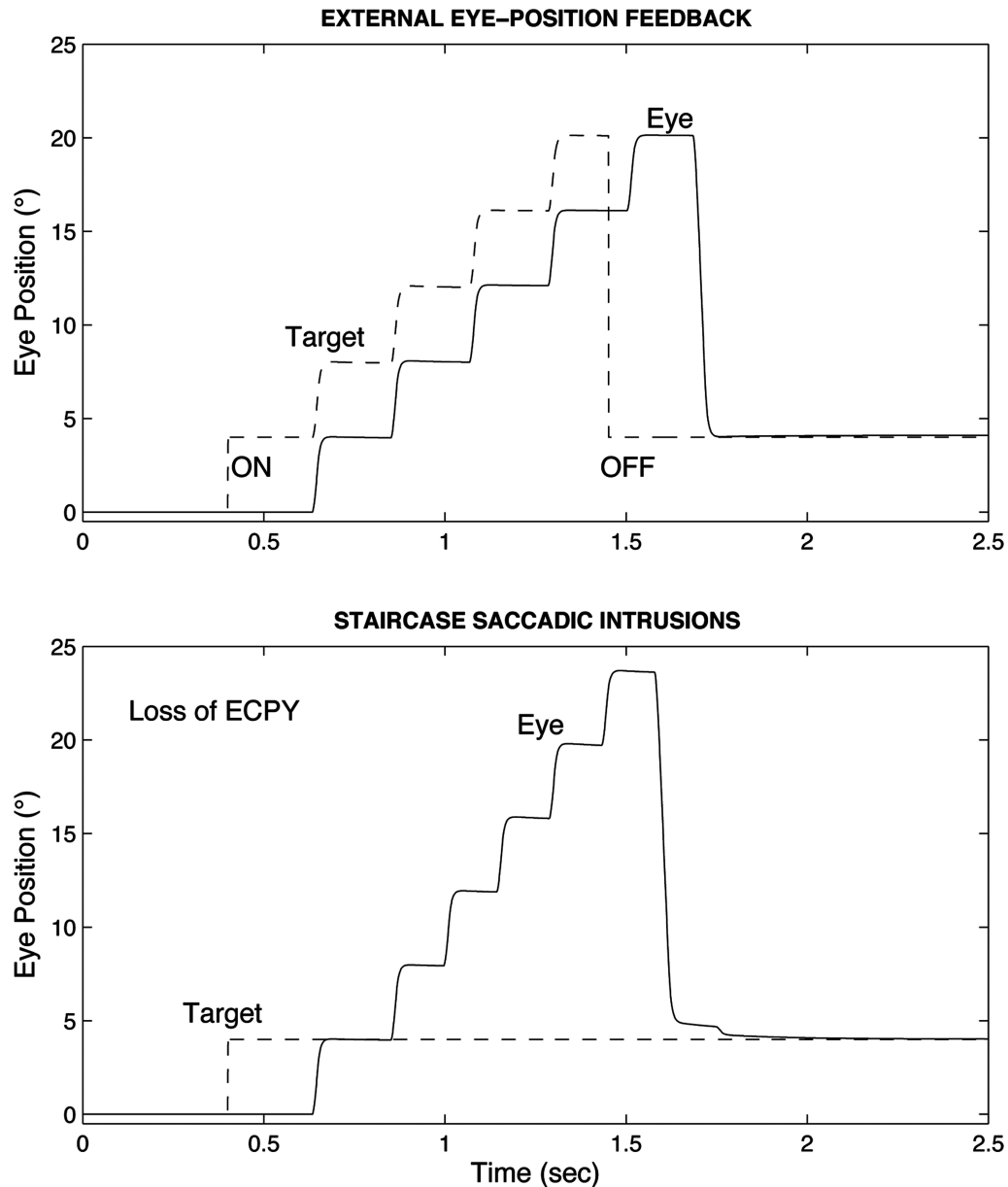


FIGURE 6 (Top) OMS model simulation of a normal individual’s ocular motor response to a step change in target position when the external gain is +1.0 (“ON”), canceling the retinal feedback gain and effectively opening the retinal feedback loop. The eye response is a “staircase” of saccades equal to the size of the target step. When the external feedback gain is reduced to 0 (“OFF”), the model’s response is a return to the original target position, simulating the response of a normal individual. The intersaccadic time intervals of the staircase response is the normal saccadic latency. (Bottom) The attempt to simulate it by a hypothetical loss of efference copy. Although superficially the same, the intersaccadic intervals following the first step past the target are shorter than the saccadic latency. This hypothetical solution *fails* to duplicate the observed responses.

reference copy is transiently disabled in an attempt to simulate SSI, the resulting staircase has intersaccadic intervals of 125 msec, the latency of internally generated corrective saccades. Thus, the loss of reference copy alone is not sufficient to simulate the SSI seen in our patient. We found that the correct simulation of SSI (i.e., with 250 msec intersaccadic intervals) required that two conditions be met: 1) a transient loss of retinal position information, e and 2) a transient change in

sampled, reconstructed retinal-error, e'^* . Figure 7 shows examples of SSI simulated by these two simultaneous dysfunctions.

Square-Wave Jerks/Oscillations (SWJ/SWO)

Because our patient exhibited SWJ and SWO in isolation and in conjunction with the SSI, we also simulated these conditions. We found that a transient change in reconstructed target-position signal, T' (caused by noise

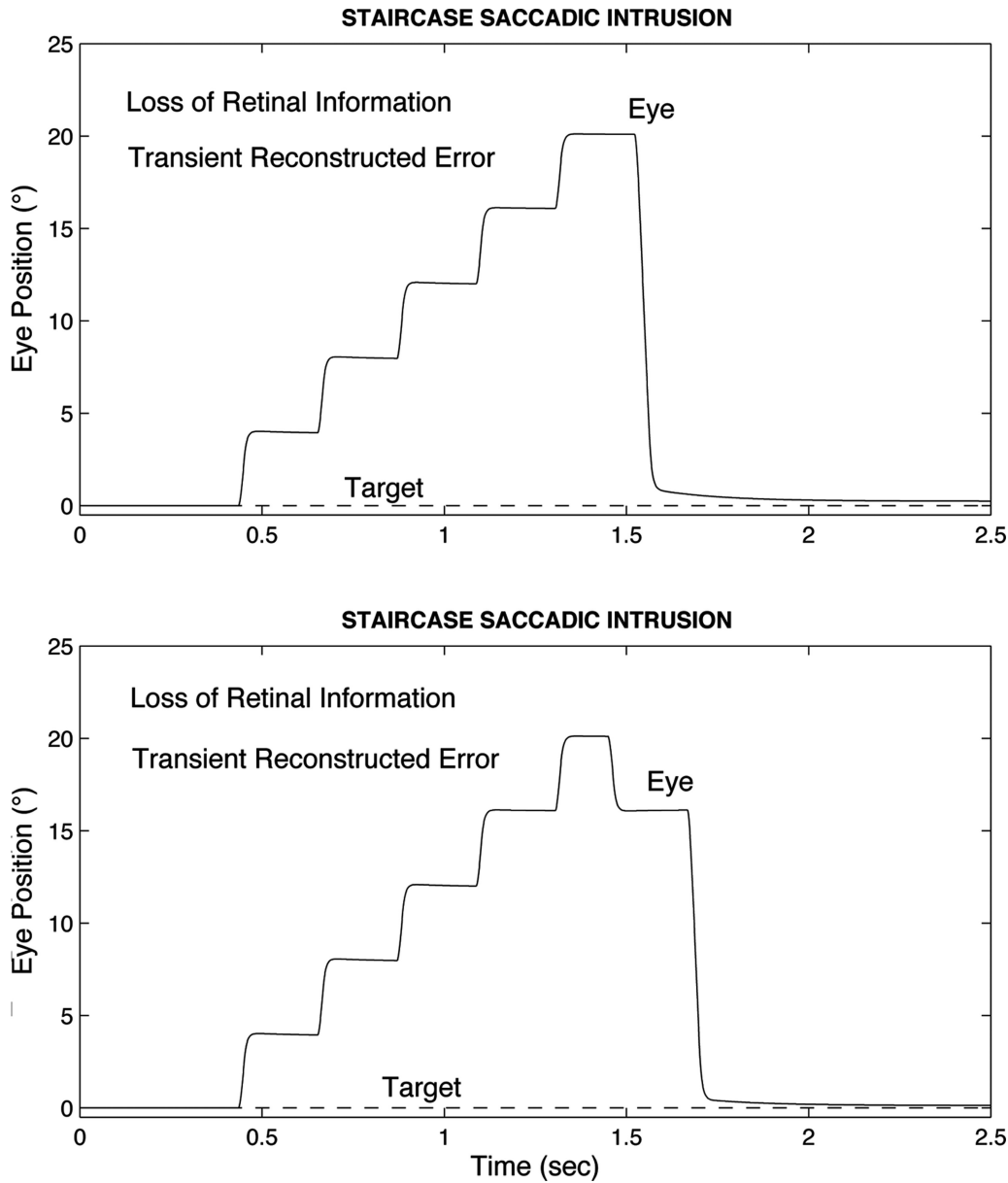


FIGURE 7 OMS model simulations of the equal-step staircase resulting from opening the retinal feedback loop by a hypothetical loss of retinal information and transient reconstructed error followed by the return saccade when the deficit is removed. The intersaccadic intervals in these simulations are equal to the saccadic latency. The nature of the saccadic return to the target is dependent on the timing of the removal of the deficit. These simulations duplicate the observed responses.

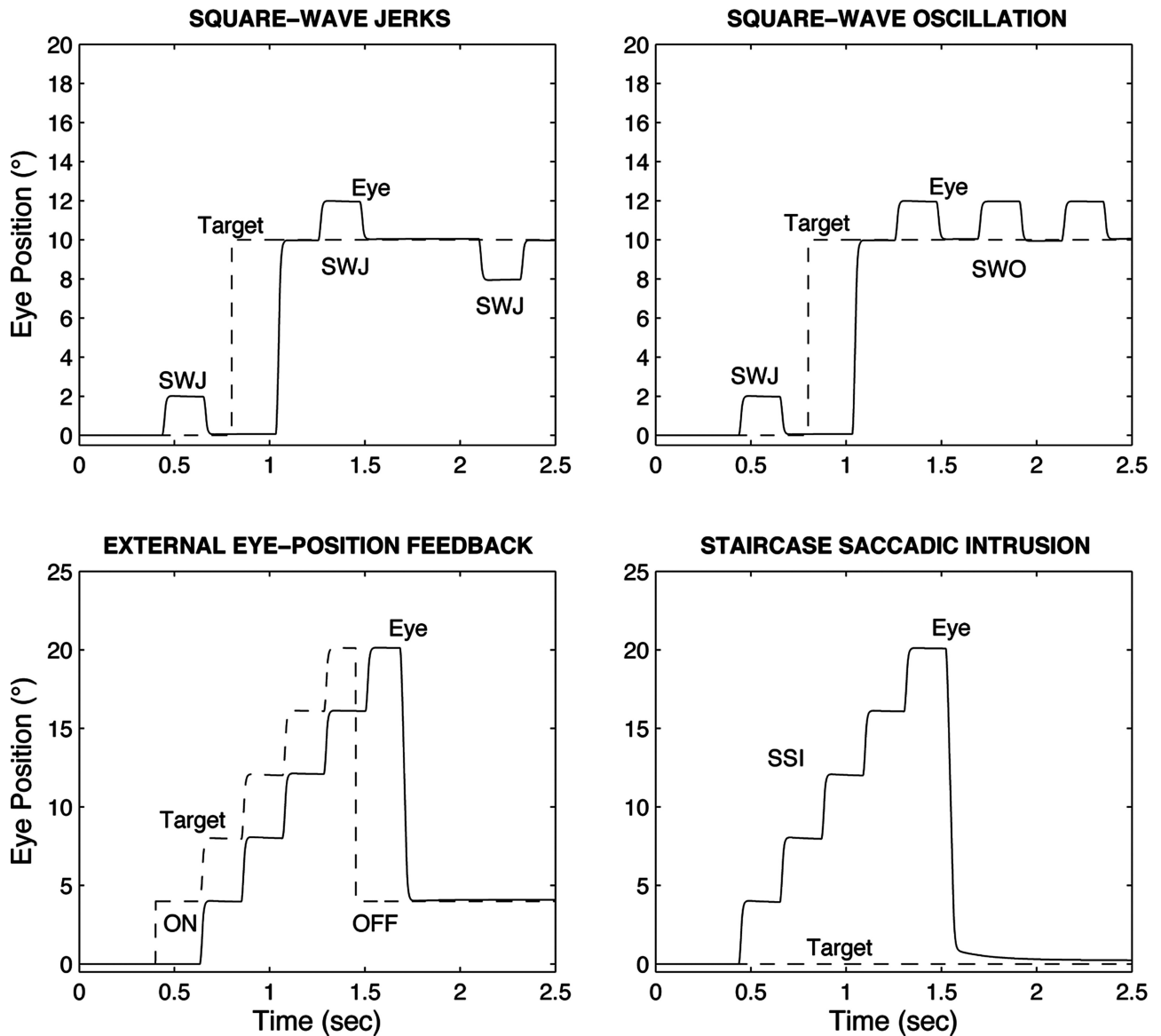


FIGURE 8 OMS model simulations of the individual components of the saccadic intrusions and oscillations found in our subject. (Top left) SWJ before and after response to a step change in target position. (Top right) SWJ before and SWO after response to a step change in target position. (Bottom left) Simulation of a rightward, equal-step SSI due to opening the retinal loop. (Bottom right) Simulation of a rightward, equal-step SSI during fixation.

or spurious signal) will produce either a SWJ or SWO, depending on the duration of the noise. Figure 8 (top left and top right) shows isolated SWJ during fixation in primary position and at 10° right as well as SWO at the latter position. Figure 8 (bottom left and bottom right) shows the simulated SSI of normals and our patient for comparison. In Figure 9 these individual intrusions and oscillations are combined in different ways to simulate the complex behavior of our patient. Note that when SWJ and SSI occurred simultaneously (bottom left and bottom right), SSI with unequal step sizes resulted, just as in our patient.

DISCUSSION

Clinical and Anatomic Correlations

Our patient demonstrates all of the abnormalities (with the exception of abnormal respiration) consistent with a diagnosis of Joubert syndrome. However, he is mildly affected and did not demonstrate the typical eye movement abnormality previously seen in Joubert syndrome.

The classic ocular motor abnormality in Joubert syndrome is ocular motor apraxia, which varies from congenital ocular motor apraxia in that both horizontal

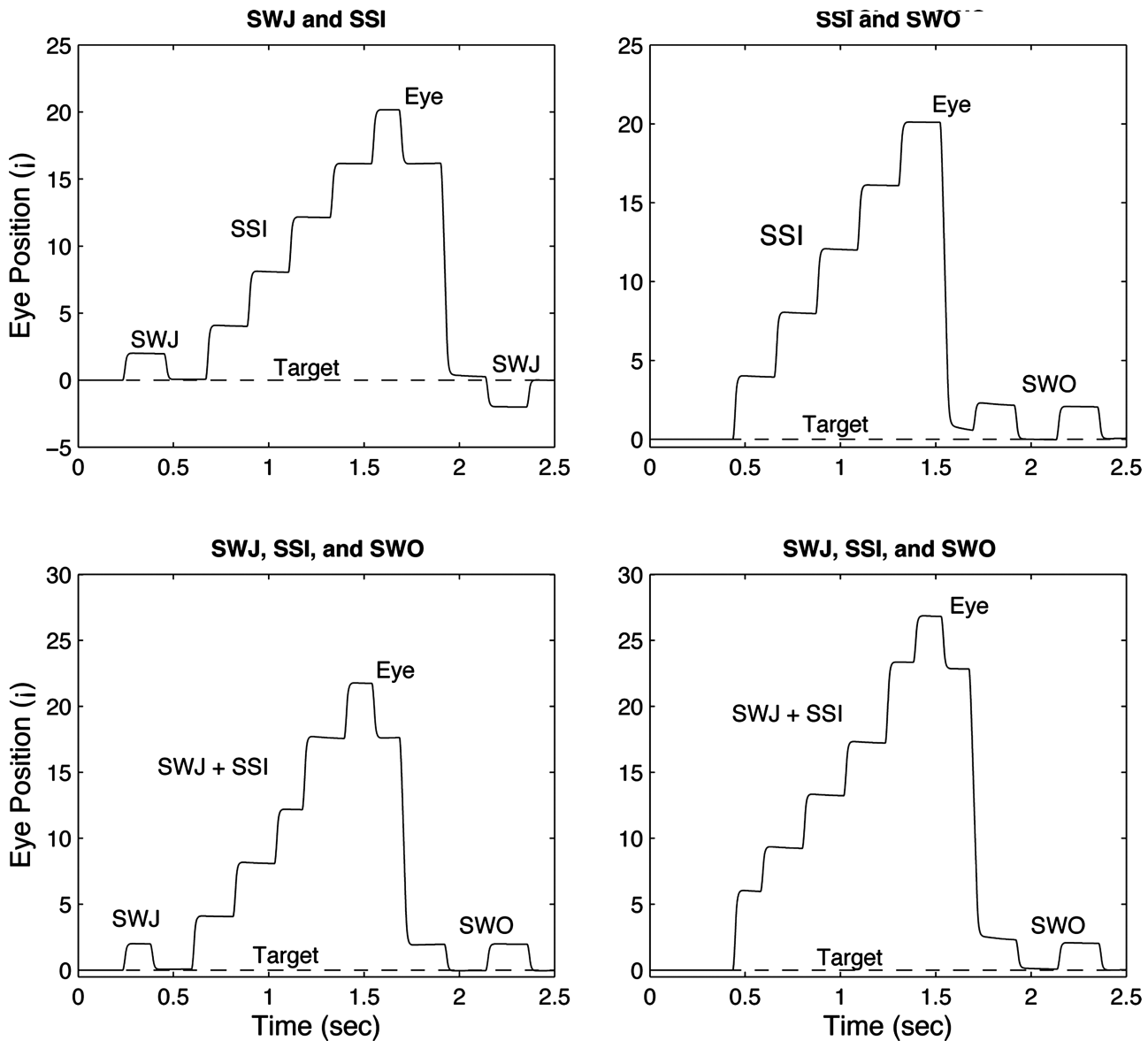


FIGURE 9 OMS model simulations of the types of saccadic intrusions and oscillations found in our subject by different combinations of their individual components. (Top left) SWJ before and after a rightward, equal-step SSI and refixation during attempted fixation. (Top right) SWO after a rightward, equal-step SSI and refixation during attempted fixation. (Bottom left) Simulation of a rightward, unequal-step SSI during fixation, preceded by a SWJ and followed by a SWO. (Bottom right) Simulation of a rightward, unequal-step SSI during fixation, followed by a SWO.

and vertical volitional saccades are affected in Joubert syndrome.¹⁰ Other identified ocular motor abnormalities in Joubert syndrome include impaired smooth pursuit with decreased gain and pendular nystagmus; our patient demonstrated the former, but not the latter.

Many ocular motor abnormalities that our patient demonstrated were consistent with cerebellar dysfunction (and not specific to Joubert syndrome); they included prominent and frequent SWJ, SWO, saccadic intrusions, ocular flutter, and impaired smooth pur-

suit (previously described in the Results section). In addition, eye drifts toward primary position from eccentric gaze suggested a neural integrator leak. All of these disorders in our patient are abnormal for children as well as adults (e.g., normal 9-year-old children make accurate saccades and pursuit). Figure 10 illustrates the sites of OMS dysfunction in the model that produced SSI and the other eye-movement abnormalities exhibited by this patient. The neuroanatomic correlate of a neural integrator leak is a lesion of either the nucleus prepositus hypoglossi or the vestibular

OMS Block Diagram: Saccadic/Pursuit Dysfunctions

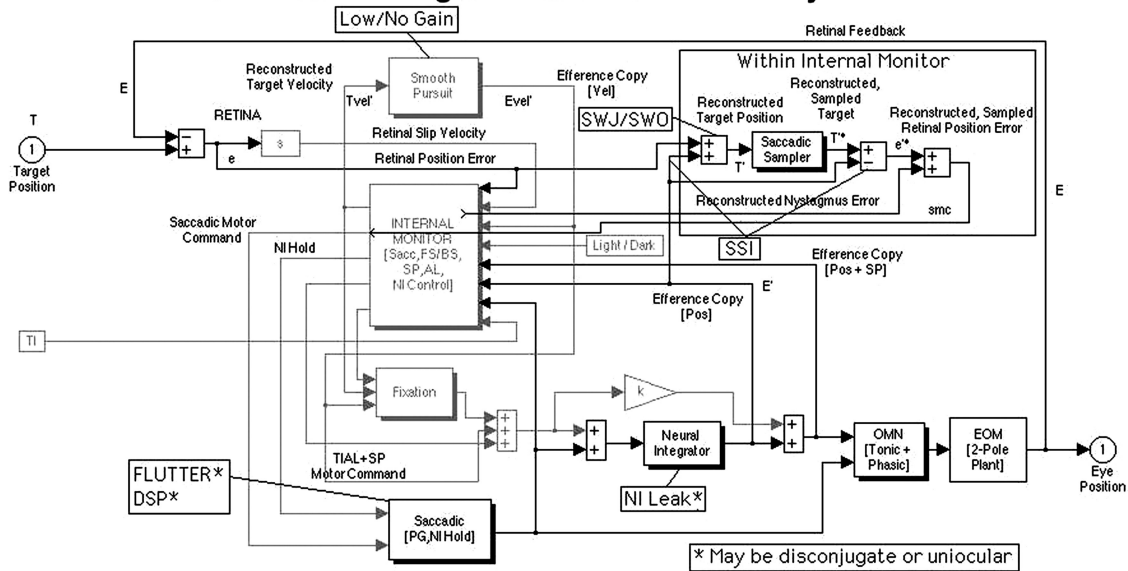


FIGURE 10 Ocular motor system (OMS) model with sites of dysfunction producing square-wave jerks/oscillations (SWJ/SWO), staircase saccadic intrusions (SSI), flutter (FLUT), double saccadic pulses (DSP), neural integrator leak (NI), or low/no-gain smooth pursuit.

nuclei in the caudal brainstem, although dysfunction of the midline cerebellum may also result in a leaky neural integrator.¹¹ Either scenario is possible in Joubert syndrome, as neuropathologic findings show not only severe hypoplasia of the cerebellar vermis, but also neuronal reduction and malformation in multiple brainstem structures.¹² Whether one agrees that this is a case of Joubert syndrome, the unique saccadic intrusions and our findings regarding the underlying mechanisms of saccadic control are more interesting and potentially important.

Ocular Motor System Model and Simulations

The behavioral OMS model simulates normal ocular motor responses, many types of ocular motor dysfunction (saccadic and nystagmus), and the ocular motor responses of individuals with those dysfunctions.^{8,9,13} Such necessarily complex models provide hypothetical mechanisms for the functions required in normal ocular motor control as well as for their dysfunction. Because they include the major functional blocks for a wide range of ocular motor responses, behavioral models are stringent test beds for new hypotheses of either subsystem control or dysfunction (i.e., how might a subsystem perform its function or how might it simulate specific dysfunction). Putative hypotheses are auto-

matically tested for undesirable or inaccurate responses and interactions with other ocular motor subsystems; simple models limited to the subsystem under study cannot provide this level of hypothesis testing. We use this behavioral model to examine how the normal saccadic subsystem (using retinal and efference-copy information to internally reconstruct target and error signals allowing accurate saccades) responds to the hypothetical mechanisms (functional sites where dysfunction occurs) we provide for various saccadic intrusions or oscillations.

Possible Mechanisms

Square-Wave Jerks/Oscillations could be simulated by transient changes in the internally reconstructed target-position signal, T' (possibly caused by noise or a spurious signal in the reconstruction or in the threshold for initiating a saccade via pause neurons). They are found in normals and in disease affecting the cerebral hemispheres and brain stem. SSI, on the other hand, required abnormalities in *two* separate ocular motor functions, loss of retinal position information plus a change in the internal sampled, reconstructed retinal error signal. This may result from transient loss of accurate retinal-error information (e), and/or sampled, reconstructed error (e'^*), plus a constant sampled, reconstructed retinal error ($e_k'^*$) that drives saccades. Saccadic

behavior is most accurately simulated using some form of sampled-data to represent the decision to make a saccade (e.g., by inhibiting pause neurons to allow the firing of burst neurons). The model demonstrated that SSI could not be simulated solely by the transient loss of accurate reconstructed eye-position information (E'), a demonstration that more limited, partial saccadic models would be incapable of. The SSI in our patient were associated with dysfunction in the superior cerebellum and vermis. This is the first occurrence of SSI that we are aware of; given the many neurological patients that we and others have recorded, we conclude SSI is a very rare disorder. It is not surprising that the more common SWJ could be simulated by a single ocular motor dysfunction, whereas SSI required a more unlikely double dysfunction. Although both functions may occur in neighboring anatomical sites, they are probably not located at the same site or SSI would be more common. Because of the complex interconnectedness of the functional blocks in this behavioral OMS model (not unlike the brain), any mechanism that accurately simulates a dysfunction without producing other, undesirable behavior emerges as a likely hypothesis.

Flutter, neural-integrator leak, and asymmetric (interocular) smooth pursuit were not simulated as part of this study; the first two have been simulated elsewhere^{14,15} and pursuit asymmetry can easily be simulated in any existing model. Flutter may be due to loss of pause-cell inhibition and may be disconjugate and has been associated with cerebellar dysfunction. Neural integrator leak may be due to loss of positive feedback around the position integrator of one eye on both sides of the brainstem if it is unidirectional and uniocular. It has been associated with dysfunction in the nucleus prepositus hypoglossi and medial vestibular nuclei. Asymmetric (directional/interocular) smooth pursuit is a difference of pursuit gains of each eye on each side of brainstem (e.g., a unilateral lesion of the pursuit pathway). It may reflect disorder in the cerebral hemispheres, thalamus, midbrain tegmentum, dorsolateral pontine nucleus, or cerebellum.

Transient loss of yoking resulted in disconjugate and uniocular saccades, disconjugate SSI and flutter, and uniocular neural-integrator leak. Frequent SWJ and SWO triggered (or coincided with) the loss of yoking and the resulting disconjugate intrusions and neural-integrator leaks. The presence of uniocular, convergent, and divergent saccades, including double saccades, in

this and other ocular motor subjects provides further evidence in support of the hypothesis that the ocular motor system is wired in a uniocular manner and therefore, due to its inherent bilateral architecture, a *unimuscular* manner.^{16–20}

Conclusions

“Staircase” saccadic intrusions are rare and our simulations demonstrate that they may result from simultaneous dysfunctions: 1) transient loss of accurate retinal-error information and/or sampled, reconstructed error; and 2) a constant sampled, reconstructed retinal error that drives saccades. This is in contrast to the more common SWJ and SWO that may be caused by a single dysfunction.

REFERENCES

- [1] Maria BL, Hoang KB, Tusa RJ, et al. “Joubert syndrome” revisited: key ocular motor signs with magnetic resonance imaging correlation. *J Child Neurol.* 1997; 12:423–430.
- [2] Maria BL, Quisling RG, Rosainz LC, et al. Molar tooth sign in Joubert syndrome: clinical, radiologic, and pathologic significance. *J Child Neurol.* 1999; 14:368–376.
- [3] Quisling RG, Barkovich AJ, Maria BL. Magnetic resonance imaging features and classification of central nervous system malformations in Joubert syndrome. *J Child Neurol.* 1999; 14:628–672.
- [4] Joubert M, Eisenring JJ, Robb JP, Andermann F. Familial agenesis of the cerebellar vermis. A syndrome of episodic hyperpnea, abnormal eye movements, ataxia, and retardation. *Neurology.* 1969; 19:813–825.
- [5] Saraiva JM, Baraitser M. Joubert syndrome: a review. *Am J Med Genet.* 1992; 43:726–31.
- [6] Steinlin M, Schmid M, Landau K, Boltshauser E. Follow-up in children with Joubert syndrome. *Neuropediatrics.* 1997; 28:204–211.
- [7] Maria BL, Boltshauser E, Palmer SC, Tran TX. Clinical features and revised diagnostic criteria in Joubert syndrome. *J Child Neurol.* 1999; 14:583–591.
- [8] Dell’Osso LF, Jacobs JB. A normal ocular motor system model that simulates the dual-mode fast phases of latent/manifest latent nystagmus. *Biological Cybernetics.* 2001; 85:459–471.
- [9] Jacobs JB, Dell’Osso LF. Congenital nystagmus: hypothesis for its genesis and complex waveforms within a behavioral ocular motor system model. *JOV.* 2004; 4:604–625.
- [10] Tusa RJ, Hove MT. Ocular and oculomotor signs in Joubert syndrome. *J Child Neurol.* 1999; 14:621–627.
- [11] Leigh RJ, Zee DS. *The Neurology of Eye Movements, Edition 3 (Contemporary Neurology Series).* New York: Oxford University Press, 1999:1–646.
- [12] Yachnis AT, Rorke LB. Neuropathology of Joubert syndrome. *J Child Neurol.* 1999; 14:655–672.
- [13] Dell’Osso LF. Nystagmus basics. Normal models that simulate dysfunction. In: Hung GK, Ciuffreda KJ, editors. *Models of the Visual System.* New York: Kluwer Academic / Plenum Publishers, 2002:711–739.
- [14] Zee DS, Robinson DA. A hypothetical explanation of saccadic oscillations. *Ann Neurol.* 1979; 5:405–414.
- [15] Abel LA, Dell’Osso LF, Daroff RB. Analog model for gaze-evoked nystagmus. *IEEE Trans Biomed Engng.* 1978; BME(25):71–75.

- [16] Helmholtz H. *Handbuch der Physiologischen Optik*. Leipzig: Voss, 1867:1–1955.
- [17] Dell’Osso LF. Evidence suggesting individual ocular motor control of each eye (muscle). *J Vestib Res*. 1994; 4:335–345.
- [18] King WM, Mays LE, Paige GD, King WM, Tweed D. Symposium. Binocular coordination of eye movements. *Soc Neurosci Abstr*. 1997; 23:1937.
- [19] King WM, Zhou W. New ideas about binocular coordination of eye movements: Is there a chameleon in the primate family tree? *Anat Rec (New Anat.)*. 2000; 261:153–161.
- [20] King WM, Zhou W. Neural basis of disjunctive eye movements. In: Kaminski HJ, Leigh RJ, editors. *Neurobiology of Eye Movements. From Molecules to Behavior—Ann NY Acad Sci* 956. New York: NYAS, 2002:273–283.